Thermochimica Acta 480 (2008) 1–9

Contents lists available at ScienceDirect

Thermochimica Acta

journal homepage: www.elsevier.com/locate/tca

Thermodynamic analysis of a combined gas turbine power system with a solid oxide fuel cell through exergy

Y. Haseli, I. Dincer*, G.F. Naterer

Faculty of Engineering and Applied Science, University of Ontario Institute of Technology, 2000 Simcoe Street North, Oshawa, Ontario, Canada, L1H 7K4

ARTICLE INFO

Article history:
Received 4 June 2008
Received in revised form 7 September 2008
Accepted 9 September 2008
Available online 18 September 2008

Keywords:
GT–SOFC cycle
Exergy
Energy
Efficiency
Exergy destruction
Thermodynamics

ABSTRACT

This paper examines the exergetic performance of a high-temperature solid oxide fuel cell (SOFC) combined with a conventional recuperative gas turbine (GT) plant. Individual models are developed for each component, specifically for SOFC and a combustor that is located downstream of the cell stack. The exergy destruction and efficiency of each component are derived and presented. Furthermore, the overall system is analyzed and its exergy efficiency, as well as exergy destruction, is computed. An assessment of the cycle is performed for an actual system and the results for certain operating conditions are compared with past published results. The comparisons provide useful verification of the thermal simulations in the present work. Further outcomes indicate that increasing the turbine inlet temperature (TIT) results in decreasing the exergy and thermal efficiencies of the cycle, whereas it improves the total specific power output. Also, an increase in either TIT or compression ratio (r_p) leads to a higher rate of exergy destruction of the plant. A comparison between the GT–SOFC plant and a traditional GT cycle, based on identical operating conditions, is also made. The superior performance of a GT–SOFC, in terms of thermal and exergy efficiencies, over a traditional GT cycle is evident: 26.6% and 27.8% better exergetic and energetic performance, respectively, than a traditional GT plant. In this case, the exergy and thermal efficiencies of the integrated cycle become as high as 57.9% and 60.6%, respectively, at the optimum compression ratio.

1. Introduction

The concept of using a gas turbine power plant (GTPP) in an integrated cycle with a solid oxide fuel cell (SOFC) has been well known for many years. A literature survey indicates that the concept was initially analyzed by Ide et al. [1], who compared the net plant efficiencies of three types of fuel cell power generation systems, including an SOFC, operated at an elevated pressure that consisted of a natural gas reformer, a fuel cell unit and a power recovery gas turbine. The efficiency losses of power generation processes are largely due to the highly irreversible fuel combustion. This efficiency can be improved if immediate contact between air and fuel is prevented, as it occurs in fuel cells [2].

Theoretical studies of combined SOFC and gas turbine (SOFC–GT) cycles have attracted increasing attention worldwide by researchers. There are several other previous works in the literature involving the thermodynamics analysis, design and performance modeling. A comprehensive study was carried out by Massardo and Lubelli [3], who investigated the performance of internal reforming solid oxide fuel cell (IRSOFC) and GT combined cycles. They developed a mathematical model that simulated the fuel cell steady-state operation.

Costamagna et al. [4] examined the design and analysis of a hybrid system (HS), based on the coupling between a recuperative microgas turbine (MGT) with a high-temperature SOFC reactor. The SOFC performance was presented and discussed. Additional past work on modeling and performance analysis of hybrid systems was documented by Chan et al. [5,6], Calise [7], Yang et al. [8], Araki et al. [9], Park et al. [10] and Granovskii et al. [11]. Most of these past works emphasize the modeling of SOFC performance. A recent study by Granovskii et al. [11] has included the exergy analyses for two SOFC–gas turbine systems to determine their efficiencies and capabilities of generating power at different rates of oxygen transport through the SOFC electrolyte (ion conductive membrane). Moreover, in past work of Cocco and Tola [12], a comparative performance analysis of SOFC–MGT power plants fuelled by methane and methanol was reported. A useful set of correlations was developed to allow direct evaluation of the voltage of the SOFC stack under known operating conditions.

As mentioned earlier, the thermal efficiency of a traditional GT plant has significant losses due to the high irreversibility within the combustion chamber. A fuel cell GT hybrid system represents an emerging technology for power generation, because of its higher

* Corresponding author.
E-mail addresses: yousef.haseli@mycampus.uoit.ca (Y. Haseli), ibrahim.dincer@uoit.ca (I. Dincer), greg.naterer@uoit.ca (G.F. Naterer).

0040-6031/$ – see front matter © 2008 Elsevier B.V. All rights reserved.
doi:10.1016/j.tca.2008.09.007

Nomenclature

A	constant in Eq. (7)
A_c	cell area (cm^2)
B	constant in Eq. (9)
E	Nernst potential or open circuit voltage (V)
e_f^{CH}	chemical exergy of fuel (kJ/kg)
e_f^{PH}	physical exergy of fuel (kJ/kg)
e_x	specific exergy flow (kJ/kg)
E^0	ideal cell voltage at standard conditions (V)
$\dot{E}_{x,dest}$	exergy destruction rate (kW)
F	Faraday constant (96485 C/mole)
h	Enthalpy (kJ/kg)
I	current (mA)
j	current density (mA/cm^2)
j_0	exchange current density (mA/cm^2)
j_1	limiting current density (mA/cm^2)
LHV	lower heating value (kJ/kg)
$\dot{m}$	mass flow rate (kg/s)
P	pressure (kPa)
$\dot{Q}$	heat transfer rate (kW)
$\dot{Q}_{Gen,FC}$	heating rate generated within the cell stack (kW)
R	universal gas constant (8.314 J/mole K)
r_p	compression ratio
STCR	ratio of number of moles of steam to carbon
T	temperature (K)
TIT	turbine inlet temperature (K)
T_o	reference temperature (K)
T_{sink}	cold sink temperature (K)
U_f	fuel utilization factor
V	voltage (V)
$\dot{W}$	power (kW)
$\dot{W}_{FC,dc}$	DC power output of the cell stack (kW)
$\dot{W}_{net}$	net power output of the plant (kW)

Greek letters

γ	ratio of specific heats
ΔV_{loss}	sum of the voltage losses due to irreversibilities
η	efficiency
λ	stoichiometric

Superscript

cyc	cycle

Subscripts

act	activation
c	cell
Comb	combustor
conc	concentration
ex	exergy
FC	fuel cell
Gen	generator
in	inlet
invert	DC–AC inverter
ohm	ohmic
out	outlet
PT	power turbine
th	thermal

energy conversion efficiency, low environmental pollution and potential use of renewable energy sources as fuels [13]. Various values have been reported for the thermal efficiency of such systems in the archival literature. They vary depending upon the configuration and proposed layout of the hybrid system. However, a review of past work indicates an efficiency of up to 60% can be achieved with an integrated cycle. Table 1 summarizes different values of thermal efficiency, which are obtained from studies of different researchers.

To the best knowledge of the authors, however, there is very limited data involving the exergy performance of such systems. Examples are past works of Calise et al. [7,20], Granovskii et al. [11] and Rao and Samuelsen [17]. In contrast to their past work, this paper aims at performing an exergy analysis of a recuperative GT combined with an SOFC. The integrated GT–SOFC layout is schematically depicted in Fig. 1. It is composed of six components: (1) air compressor, (2) recuperator, (3) high-temperature solid oxide fuel cell (SOFC), (4) combustor, (5) gas turbine, and (6) power turbine. The corresponding temperature-entropy diagram of the process is shown in Fig. 2, in which typical values of mass flow rate, temperature and pressure of the working fluid at various points of a GT–SOFC plant, operating at the optimum point, are also given. Energy and exergy balance equations of each component will be derived and then linked. Furthermore, energy and exergy balance equations of the entire system are obtained, based on our earlier paper [30], which looks into the combined system from the entropy generation viewpoint. The current study allows us to investigate effects of various performance parameters, such as the compression ratio (r_p) and turbine inlet temperature, on the thermal and exergy efficiencies. The analysis also enables us to observe the contribution of each component to the total irreversibilities of the system.

2. Energy and exergy formulations of system components

The thermodynamic performance of each of the components in the preceding section will be analyzed in this section. The energy and exergy balance equations are derived under the assumption of steady flow for the entire cycle. The main stream of the working fluid at different states of the cycle is shown in Fig. 2 (states 1–8). Air is approximated as an ideal gas.

2.1. SOFC

The fuel utilized to supply the system is methane (CH_4), with a lower heating value of 50,050 kJ/kg [23]. The following electrochemical reactions occur within the anode and cathode of the fuel cell (e.g., [24,25]):

$$\text{Anode}: \begin{array}{l} H_2 + O^{=} \rightarrow H_2O + 2e^{-} \\ CO + O^{=} \rightarrow CO_2 + 2e^{-} \\ CH_4 + 4O^{=} \rightarrow 2H_2O \rightarrow +CO_2 + 8e^{-} \end{array} \quad (1a)$$

$$\text{Cathode}: \tfrac{1}{2}O_2 + 2e^{-} \rightarrow O^{=} \quad (1b)$$

In practice, insignificant direct oxidation of the CO and CH_4 may occur. It is common in a system analysis to assume that H_2 is produced by CO and CH_4 reacting, at equilibrium, with H_2O through the water gas shift and steam reforming reactions, respectively. The direct oxidation can be important under certain conditions, such as the entrance of a fuel cell. The degree to which an anode supports direct oxidation will then impact the degree of pre-reforming of the fuel that is required, which in turn typically impacts the balance of plant complexity and cost [24].

The net cell reaction is thus written as

$$CH_4 + 2O_2 \rightarrow CO_2 + 2H_2O \quad (2)$$

The solution of the overall mass and energy balances of the fuel cell requires the evaluation of both the voltage and the current

Table 1
Survey of thermal efficiencies of combined SOFC-GT plants in past literature.

Efficiency	System configuration	Reference
68.1	Pressurized cycle using an SOFC and integrated GT bottoming cycle	Harvey and Richter [2]
60.0	Gasification process linked with an SOFC and GT	Lobachyov and Richter [14]
70<	Pressurized SOFC–GT cycle with a heat recovery bottoming cycle	Campanari and Macchi [15]
60<	Recuperated microgas turbine (MGT) with a high-temperature SOFC	Costamagna et al. [4]
60<	SOFC stack, combustor, GT, two compressors and 3 recuperators	Chan et al. [5]
60.0	50 kW microturbine coupled with a high-temperature SOFC	Massardo et al. [16]
66.2	Pressurized tubular SOFC combined with an intercooled-rehear GT	Rao and Samuelsen [17]
69.1	Humid air turbine (HAT) cycle incorporated with the above cycle	Rao and Samuelsen [17]
76	Dual SOFC-HAT hybrid cycle	Rao and Samuelsen [17]
60<	Internal-reforming (IR) SOFC–GT power generation system	Chan et al. [6]
70.6	Combined SOFC-GT system with liquefaction recovery of CO_2	Inui et al. [18]
65.0	30-kW μGT–SOFC hybrid system	Uechi et al. [19]
65.4	IR tubular SOFC-GT plant with 3 heat exchangers and mixers	Calise et al. [7]
60.0	1.5 MW integrated IRSOFC with two GTs and one HRSG	Calise et al. [20]
56.1	Two-staged low and high-temperature SOFC power generation cycle	Araki et al. [9]
68.5	Multi-staged SOFC/gas turbine/CO_2 recovery power plant	Araki et al. [21]
59.4	Recuperated GT integrated with SOFC	Tse et al. [22]
68.7	Recuperated GT with compressor air intercooling and two SOFCs	Tse et al. [22]

produced by the stack. The reversible cell voltage, E, is defined by the Nernst equation as (e.g., [24,25])

$$E = E^0 + \frac{RT}{8F} \ln\left(\frac{P_{CH_4} P_{O_2}^2}{P_{CO_2} P_{H_2O}^2}\right) \quad (3)$$

where E^0 is the ideal cell voltage at standard conditions (i.e., 298.15 K and 1 bar), R is the universal gas constant, T is the stack temperature, and F denotes the Faraday constant (96,485 C/mole). The Nernst equation provides a relationship between the ideal standard potential, i.e. E^0, for the cell reaction and the ideal equilibrium potential, i.e., E, at other temperatures and partial pressures of reactants and products. Once the ideal potential at standard conditions is known, the ideal voltage can be determined at other temperatures and pressures through Eq. (3). Typical ideal voltage values for an intermediate-temperature SOFC operating at 800 °C and a high-temperature SOFC operating at 1100 °C are 0.99 V and 0.91 V, respectively [24,25]. The calculated fuel cell voltage from Eq. (3) is obtained for an open circuit system. When the current produced by the cells is used for the external load, additional losses must be taken into account.

By defining the current density, j, as the rate of electron transfer per unit activation area of the fuel cell, the DC electric power produced by the fuel cell can be expressed by

$$\dot{W}_{FC,dc} = V_c j A_c \quad (4)$$

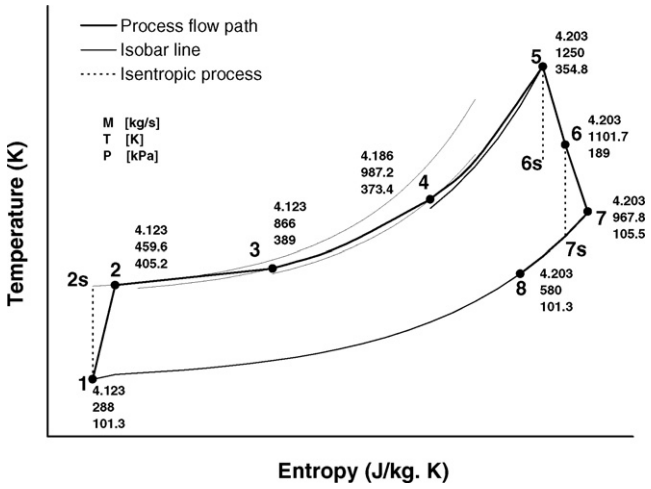

Fig. 2. T–S diagram of a GT–SOFC cycle corresponding to Fig. 1.

where V_c represents the cell voltage, which is the difference between the open-circuit voltage, obtained from Nernst equation, and voltage losses in the fuel cell, i.e.,

$$V_c = E - \Delta V_{loss} \quad (5)$$

where ΔV_{loss} is the sum of the voltage losses due to irreversibilities in the fuel cell that include activation polarization, ohmic losses and

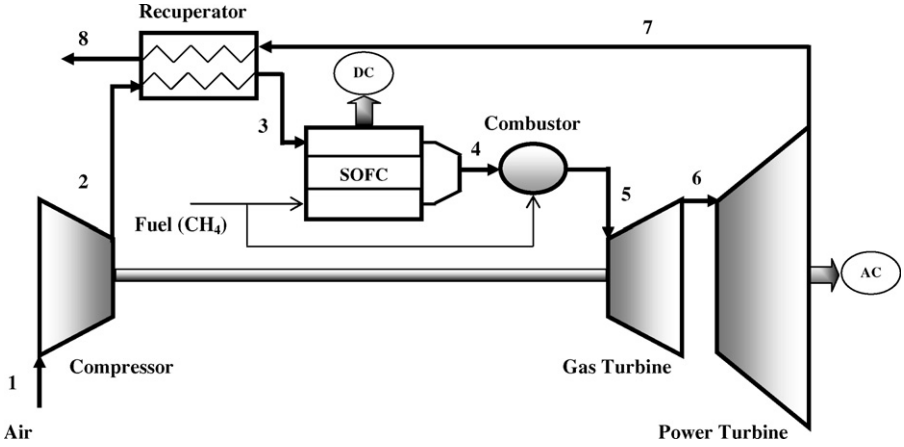

Fig. 1. Schematic of combined gas turbine power plant with SOFC.

concentration losses.

$$\Delta V_{\text{loss}} = V_{\text{act}} + V_{\text{ohm}} + V_{\text{conc}} \tag{6}$$

$$V_{\text{act}} = A \ln\left(\frac{j}{j_0}\right) \tag{7}$$

$$V_{\text{ohm}} = jr \tag{8}$$

$$V_{\text{conc}} = -B \ln\left(1 - \frac{j}{j_1}\right) \tag{9}$$

The constant A is higher for an electrochemical reaction that is slow and it is proportional to temperature. The current density, j_0, is the current density at which the overvoltage begins to move from zero [26]. The current density is given in units of mAcm^{-2}, so the area-specific resistance, r, is given in $\text{k}\Omega\,\text{cm}^2$. Eq. (7) is, for instance, utilized in the of Calise et al. [20] and Kuchonthar et al. [27] to evaluate activation loss, whereas Chan et al. [5], Calise et al. [20] and Kuchonthar et al. [27] have used Eq. (9) for determining the concentration loss in their studies.

At a high operating temperature of the SOFC, the concentration loss can be neglected because diffusion is a very efficient process. Massardo and Lubelli [3] provided correlations to evaluate polarization and ohmic losses, which were employed in a recent study by Park et al. [10]. The actual cell voltage V_c depends upon operating parameters like the current density, operating pressure and temperature, etc. The Fuel Cell Handbook [24] includes empirical correlations that relate the performance of an SOFC to these parameters. For example, the following equation approximates the effect of pressure on cell performance at 1000 °C:

$$\Delta V_{\text{P}}(\text{mV}) = 59 \ln\left(\frac{P_2}{P_1}\right) \tag{10}$$

where P_1 and P_2 are different cell pressures. In addition, the dependence of the SOFC performance on temperature is expressed by

$$\Delta V_{\text{T}}(\text{mV}) = 0.008(T_2 - T_1)j \tag{11}$$

These equations are useful tools to evaluate the actual cell voltage at various operating conditions.

There will be some heat generation within the cell stack, due to the irreversibilities mentioned earlier. The following equation may be used to determine the rate of heat generated within the cell stack:

$$\dot{Q}_{\text{Gen,FC}} = I\Delta V_{\text{loss}} = jA_c(E - V_c) \times 10^{-6} \quad [\text{kW}] \tag{12}$$

The oxygen used in the reaction of Eq. (2) will be normally derived from air. The airflow is usually well above the stoichiometric amount, typically twice higher. If the stoichiometric ratio is λ, then the following equation gives the mass flow rate of air usage (e.g., [26]):

$$\text{Air usage} = 3.57 \times 10^{-7} \times \lambda \times \frac{\dot{W}_{\text{FC,dc}}}{V_c} \quad [\text{kg/s}] \tag{13}$$

The mass balance for this system gives

$$\sum_{\text{in}} \text{mass flows} = \sum_{\text{out}} \text{mass flows} \tag{14}$$

Thus,

$$\dot{m}_3 + \dot{m}_{\text{fuel,FC}} = \dot{m}_4 = \dot{m}_3 + \dot{m}_{\text{fuel,FC}} \times U_f + \dot{m}_{\text{fuel,FC}} \times (1 - U_f) \tag{15}$$

where U_f denotes the fuel utilization factor, so that the last term on the right side of the above equality represents the non-reacted mass flow rate that leaves the fuel cell downstream of the products. We can now apply the first law of thermodynamics to the SOFC, assuming an adiabatic process, which yields

$$\dot{m}_3 h_3 + \dot{m}_{\text{fuel,FC}} \times U_f \times \text{LHV} + \dot{m}_{\text{fuel,FC}} \times (1 - U_f) h_{\text{fuel,in}} - \dot{W}_{\text{FC,dc}} - \dot{m}_4 h_4 = 0 \tag{16}$$

where LHV is the lower heating value of the fuel. Additionally, we can proceed with one more step to write the exergy balance equation of the SOFC as follows:

$$\dot{m}_3 e_{x3} + \dot{m}_{\text{fuel,FC}} e_f^{\text{PH}} + \dot{m}_{\text{fuel,FC}} U_f e_f^{\text{CH}} - \dot{m}_4 e_{x4} - \dot{W}_{\text{FC,dc}} - \dot{E}_{\text{x,dest,FC}} = 0 \tag{17}$$

where e_f^{PH} and e_f^{CH} denote, respectively, the physical and chemical exergy of the fuel utilized.

Hence, the exergy efficiency of the cell is evaluated as follows:

$$\eta_{\text{ex,FC}} = \frac{\dot{W}_{\text{FC,dc}}}{(\dot{m}_{\text{fuel,FC}} e_f^{\text{PH}} + \dot{m}_{\text{fuel,FC}} U_f e_f^{\text{CH}}) - (\dot{m}_4 e_{x4} - \dot{m}_3 e_{x3})} \tag{18}$$

2.2. Combustor

The working fluid of the cycle with products from the fuel cell is further heated within the combustor. Considering that non-reacted flow of fuel from the SOFC is burnt in the combustor, the mass balance of the combustor yields

$$(\dot{m}_3 + \dot{m}_{\text{fuel,FC}} U_f) + \dot{m}_{\text{fuel,FC}}(1 - U_f) + \dot{m}_{\text{fuel,Comb}} = \dot{m}_4 + \dot{m}_{\text{fuel,Comb}} = \dot{m}_5 \tag{19}$$

The first law of thermodynamics for the combustor can be expressed as

$$(\dot{m}_3 + U_f \times \dot{m}_{\text{fuel,FC}}) h_4 + \dot{Q}_{\text{Comb}} - \dot{m}_5 h_5 - \dot{Q}_{\text{loss}} = 0 \tag{20}$$

where

$$\dot{Q}_{\text{Comb}} = [\dot{m}_{\text{fuel,FC}} \times (1 - U_f) + \dot{m}_{\text{fuel,Comb}}] \times \text{LHV} \tag{21}$$

$$\dot{Q}_{\text{loss}} = [\dot{m}_{\text{fuel,FC}} \times (1 - U_f) + \dot{m}_{\text{fuel,Comb}}] \times (1 - \eta_{\text{Comb}}) \times \text{LHV} \tag{22}$$

and η_{Comb} represents the efficiency of the combustor.

The exergy balance equation can be written as

$$\dot{m}_4 e_{x4} + \dot{m}_{\text{fuel,FC}} \times (1 - U_f) e_f^{\text{CH}} + \dot{m}_{\text{fuel,Comb}}(e_f^{\text{PH}} + e_f^{\text{CH}}) - \dot{m}_5 e_{x5} - \left(1 - \frac{T_o}{T_{\sin k}}\right) \dot{Q}_{\text{loss}} - \dot{E}_{\text{x,dest,Comb}} = 0 \tag{23}$$

The fifth term on the left side of the above equation (exergy rate due to the heat lost) will be zero when $T_o = T_{\sin k}$. The exergy efficiency of the combustor can be now written as

$$\eta_{\text{ex,Comb}} = \frac{\dot{m}_5 e_{x5} - \dot{m}_4 e_{x4}}{\dot{m}_{\text{fuel,FC}} \times (1 - U_f) e_f^{\text{CH}} + \dot{m}_{\text{fuel,Comb}}(e_f^{\text{PH}} + e_f^{\text{CH}})} \tag{24}$$

2.3. Formulations for the compressor, turbine and recuperator

Thermodynamic models of the compressor, turbine and recuperator are commonly available in standard thermodynamics textbooks, such as Ref. [23]. The final equations of exergy destruction and exergy efficiencies are listed in Table 2 as part of this analysis. These equations will be utilized in the system analyses and calculations, which will be presented in Section 4.

Table 2
Exergy destruction and efficiency equations of compressor/turbine/recuperator.

Compressor	Exergy destruction	$\dot{E}_{x,dest,C} = \dot{W}_C - \dot{m}_1(e_{x2} - e_{x1})$	(25)
	Exergy efficiency	$\eta_{exe,C} = \dfrac{\dot{m}_1(e_{x2} - e_{x1})}{\dot{W}_C}$	(26)
Recuperator	Exergy destruction	$\dot{E}_{x,dest,C} = \dot{m}_7(e_{x7} - e_{x8}) - \dot{m}_3(e_{x3} - e_{x2})$	(27)
	Exergy efficiency	$\eta_{exe,Recup} = \dfrac{\dot{m}_3(e_{x3} - e_{x2})}{\dot{m}_7(e_{x7} - e_{x8})}$	(28)
Gas turbine	Exergy destruction	$\dot{E}_{x,dest,GT} = \dot{m}_5(e_{x5} - e_{x6}) - \dot{W}_{GT}$	(29)
	Exergy efficiency	$\eta_{exe,GT} = \dfrac{\dot{W}_{GT}}{\dot{m}_5(e_{x5} - e_{x6})}$	(30)
Power turbine	Exergy destruction	$\dot{E}_{x,dest,PT} = \dot{m}_6(e_{x6} - e_{x7}) - \dot{W}_{PT}$	(31)
	Exergy efficiency	$\eta_{exe,PT} = \dfrac{\dot{W}_{PT}}{\dot{m}_6(e_{x6} - e_{x7})}$	(32)

2.4. Overall balance equations for the cycle

The integrated gas turbine power plant with an SOFC in Fig. 1 may be analyzed as a control volume, as shown schematically in Fig. 3, which shows the inlet and outlet flows (including mass flow, heat and work) at the boundary of the system. The mass balance for the system is written as (see Fig. 3a):

$$\dot{m}_1 + \dot{m}_{fuel} - \dot{m}_8 = 0 \tag{33}$$

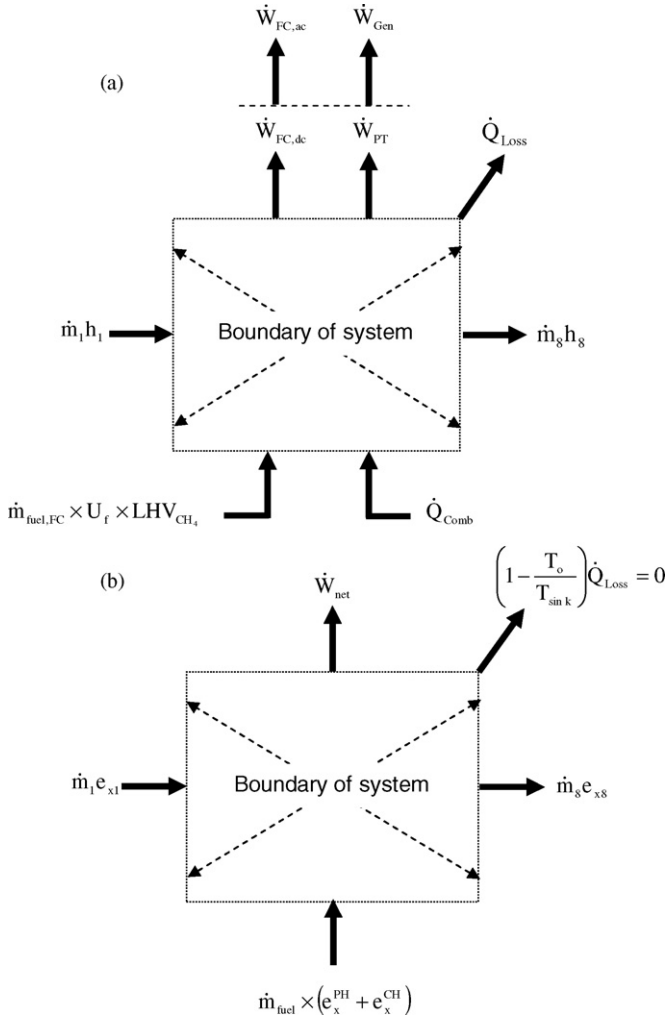

Fig. 3. GT–SOFC cycle from Fig. 1 as a control volume for the overall (a) energy balance and (b) exergy balance.

where

$$\dot{m}_1 = \dot{m}_2 = \dot{m}_3 \tag{34}$$

$$\dot{m}_{fuel} = \dot{m}_{fuel,FC} + \dot{m}_{fuel,Comb} \tag{35}$$

$$\dot{m}_8 = \dot{m}_7 = \dot{m}_6 = \dot{m}_5 \tag{36}$$

The overall energy balance of the system gives

$$\dot{m}_1 h_1 + \dot{m}_{fuel,FC} \times U_f \times LHV_{CH_4} + \dot{Q}_{Comb} - \dot{m}_8 h_8 - \dot{Q}_{loss} - \dot{W}_{FC,dc} - \dot{W}_{PT} = 0 \tag{37}$$

where $\dot{Q}_{Comb}$ and $\dot{Q}_{loss}$ are previously defined in Eqs. (21) and (22), respectively. The total thermal efficiency of the GT–SOFC plant is defined as the ratio of the network output to the total rate of energy input to the system, i.e.,

$$\eta_{th}^{cyc} = \frac{\dot{W}_{net}}{\dot{Q}_{tot}} \tag{38}$$

where

$$\dot{W}_{net} = \dot{W}_{FC,ac} + \dot{W}_{Gen} \tag{39}$$

$$\dot{W}_{FC,ac} = \eta_{invert}\dot{W}_{FC,dc} \tag{40}$$

$$\dot{W}_{Gen} = \eta_{Gen}\dot{W}_{PT} \tag{41}$$

$$\dot{Q}_{tot} = \dot{m}_{fuel,FC} \times U_f \times LHV_{CH_4} + \dot{Q}_{Comb} \tag{42}$$

Here η_{invert} denotes the DC–AC inverter efficiency and η_{Gen} represents the AC generator efficiency.

The exergy balance equation of the system can be derived in a similar manner according to Fig. 3b, which illustrates the inlet and outlet sources of exergy of the GT–SOFC cycle.

$$\dot{m}_1 e_{x1} + \dot{m}_{fuel}(e_f^{PH} + e_f^{CH}) - \dot{m}_8 e_{x8} - \dot{W}_{net} - \dot{E}_{x,dest} = 0 \tag{43}$$

The exergy destruction of the entire cycle is the sum of exergy destroyed in components from Eqs. (17), (23), (25), (27), (29) and (31), as well as exergy destruction due to inverting DC power from the fuel cell into AC power, and exergy destruction due to transmitting the turbine power output to the generator.

The exergy efficiency of the plant is the ratio of the net exergy recovered to the supplied net exergy into the system, i.e.,

$$\eta_{ex}^{cyc} = \frac{\dot{W}_{net}}{\dot{m}_{fuel}(e_f^{PH} + e_f^{CH})} \tag{44}$$

In the following section, results of these formulations will be presented and analyzed for typical operating conditions of the combined cycle.

Table 3
Main operating parameters of the GT–SOFC plant.

Gas turbine cycle	
Compressor efficiency (η_{comp})	0.81
Turbine efficiency (η_{GT})	0.84
Power turbine efficiency (η_{PT})	0.89
Recuperator effectiveness (η_{Recup})	0.8
Combustor efficiency (η_{Comb})	0.98
AC generator efficiency (η_{Gen})	0.95
Solid oxide fuel cell	
Air utilization factor (U_a)	0.25
Fuel utilization factor (U_f)	0.85
Steam-to-carbon ratio (STCR)	2.5
Stack temperature (T_{stack})	1273.15 K
Current density	0.3 A/cm^2
DC–AC inverter efficiency (η_{invert})	0.89
Cell area	834 cm^2
Pressure losses	
Recuperator gas/air sides	4%
Fuel cell stack	4%
Combustor	5%
Ambient conditions	
Temperature	288 K
Pressure	1 atm

Source: Ref. [22].

3. Results and discussion

Typical operational conditions of a combined GT–SOFC power plant are adopted from Ref. [22] and summarized in Table 3. The fuel is CH_4 with a lower heating value of 50,050 kJ/kg [23] and specific chemical exergy of 51,840 kJ/kg [28]. The combustor efficiency of 98% is the original efficiency given for the system by [27] and later employed by [30]. Although this value may seem to be on high side, it is consistent with the practical data presented in a gas turbine combustion book by Lefebvre [31]. Though some manufacturers in practice list thermal efficiencies for efficient combustors, ranging from 95% to 99% in some instances (see [32]).

In a past study by Tse et al. [27], the compression ratio (r_p) is 4, turbine inlet temperature is 1250 K, and a current density (j) of 300 mA/cm^2 are suggested as the optimal conditions for the hybrid cycle. For purposes of validation, the overall performance of the cycle predicted by the present model was compared against past values reported by Tse et al. [22]. This comparison is shown in Table 4 and fair agreement can be observed, thereby providing useful verification of the present formulation. A large difference in predicted values for the specific power output of the turbine may be due to a different method of calculating the specific heat ratio (γ), which would result in different specific powers. The computed values of mass flow rate, temperature and pressure at different points of the GT–SOFC system at optimum operation are represented in Fig. 2. From this figure, an expansion and temperature drop of about 166 kPa and 140 K, respectively, occur in the GT, in order to meet

Table 4
Comparison between the simulation results and predicted values of Tse et al. [22] for a pressure ratio (r_p) of 4 and turbine inlet temperature of 1250 K.

Parameter	Unit	Present study	Tse et al. [22]
Thermal efficiency of the plant	%	60.6	59.4
Specific power to drive compressor	kJ/kg	175.7	174
Specific power from generator	kJ/kg	146.4	158
Specific power from SOFC	kJ/kg	437.5	440
Total specific power produced	kJ/kg	583.9	598
Net power	kW	2419.3	2457.4
Air mass flow rate	kg/s	4.123	4.11
Mass flow rate of fuel to the combustor	kg/h	62.1	64
Mass flow rate of fuel to the fuel cell	kg/h	225.3	232.4

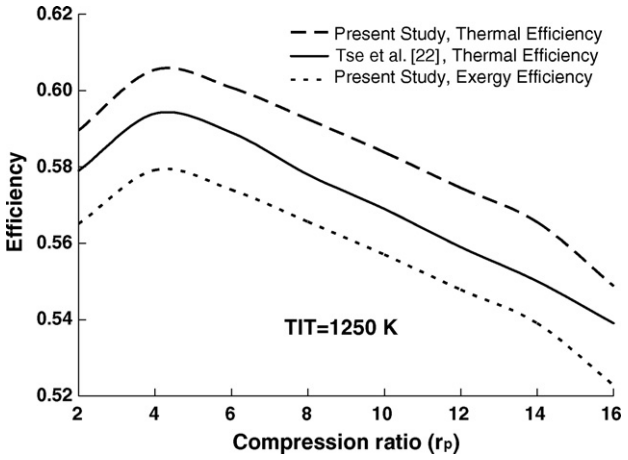

Fig. 4. Thermal and exergy efficiencies of the GT–SOFC cycle, versus compression ratio.

the work requirement of the compressor. However, from Fig. 2, the working fluid at the GT outlet still has a very high temperature with a pressure greater than atmospheric pressure. Thus, it can drive another turbine, such as a PT, to produce additional power. At the exit of the PT, the working fluid's pressure is almost atmospheric, but still with a high temperature. Therefore, before discharging it to the atmosphere, its heat is utilized to preheat the entering fresh air within a heat exchanger, i.e., recuperator.

Fig. 4 illustrates another comparison of the results between the present simulations and prediction of Tse et al. [22]. The thermal efficiencies are compared for different compression ratios. Both profiles indicate that the maximum thermal efficiency is achieved at a compression ratio of 4. The variation of exergy efficiency of the cycle versus the comparison ratio is also depicted in Fig. 4. A nearly uniform difference between the thermal and exergy efficiencies (about 2.6%) is observed over the range of compression ratios shown in Fig. 4. The exergy efficiency confirms that the optimal exergetic performance of the plant occurs at about $r_p = 4$.

The influence of ambient temperature on the GT–SOFC cycle performance is investigated. The results are indicated in Fig. 5. In colder weather, the efficiency of the cycle and the net power output are higher, mainly due to less power requirements of the compressor.

The effects of the turbine inlet temperature on the thermodynamic efficiencies and power output are shown in Fig. 6. A reduction in both thermal and exergy efficiencies is seen when the turbine inlet temperature increases. This is an interesting result which

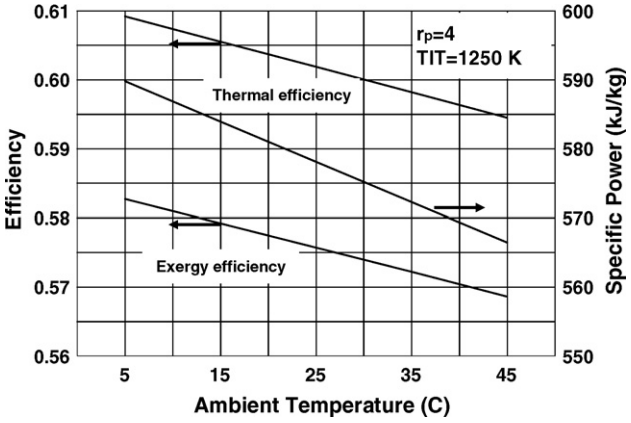

Fig. 5. Effect of ambient temperature on thermodynamic efficiencies and net specific power.

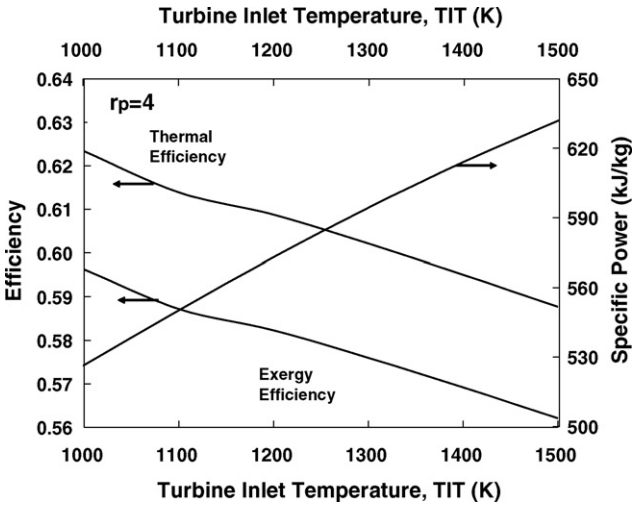

Fig. 6. Effects of turbine inlet temperature (TIT) on the thermal and exergy efficiencies, and the net power output of a GT–SOFC plant, at a compression ratio of 4.

reveals that further heating of the working fluid after the fuel cell in the combustor is not effective. However, the reason for utilizing the combustor is mainly to burn non-reacted flow of fuel in the SOFC [7,20]. Obtaining a certain power output from the cycle, as well as controlling the plant under part-load operations, are further reasons for utilization of the combustor [29]. From Fig. 6, increasing the turbine inlet temperature leads to a higher specific power output.

Fig. 7 illustrates the irreversibilities of the plant, in terms of the exergy destruction rate versus compression ratio. A higher r_p would result in larger rates of irreversibilities within the cycle, predominantly in the compressor and gas turbine. A higher r_p would require a larger amount of work drawn from the gas turbine to drive the compressor, so the irreversibility of both components would increase.

The effect of the turbine inlet temperature on the cycle irreversibility has been also investigated and selected results are depicted in Fig. 8. Providing a higher turbine inlet temperature requires an increase of the combustion heat transfer rate in the combustor, thereby increasing the flow rate of the fuel. Therefore, a higher heat transfer rate leads to a higher rate of irreversibilities.

In order to determine how much each component contributes to the total irreversibility of the plant, an illustrative example is

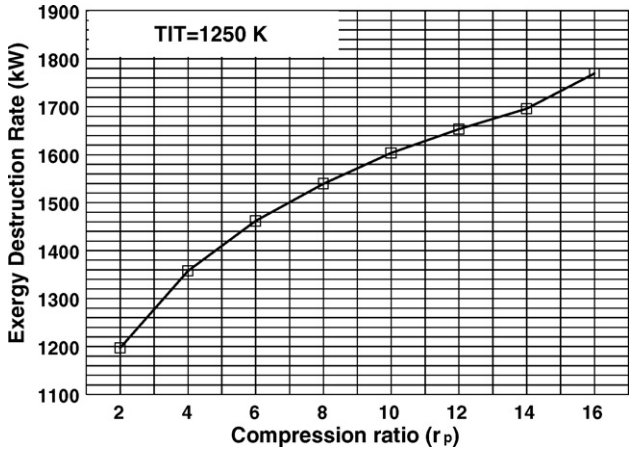

Fig. 7. Variation of the exergy destruction rate of the GT–SOFC plant, versus compression ratio.

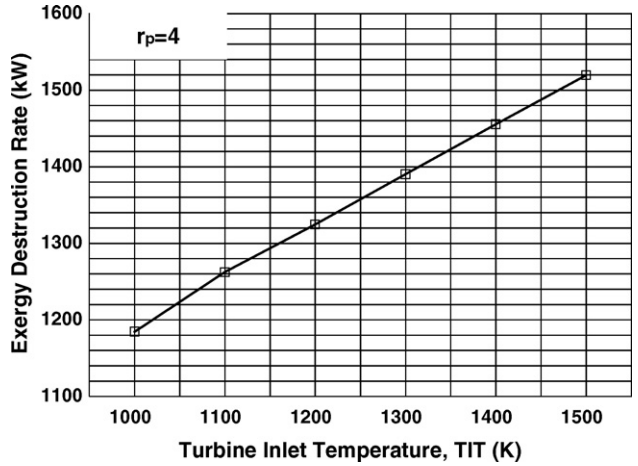

Fig. 8. Variation of the exergy destruction rate for a GT–SOFC plant versus turbine inlet temperature (TIT).

presented in Fig. 9. The exergy destroyed in each component is shown in Fig. 9(a). Furthermore, the temperature distribution along the working fluid stream from the inlet to the outlet is illustrated in Fig. 9(b). The maximum irreversibility occurs in the combustor, where the stream of gas has the highest temperature. However, not only does temperature affect the rate of irreversibility, but also other parameters such as pressure drop and reactions influence the rates of exergy destruction. From Fig. 9, the most irreversible

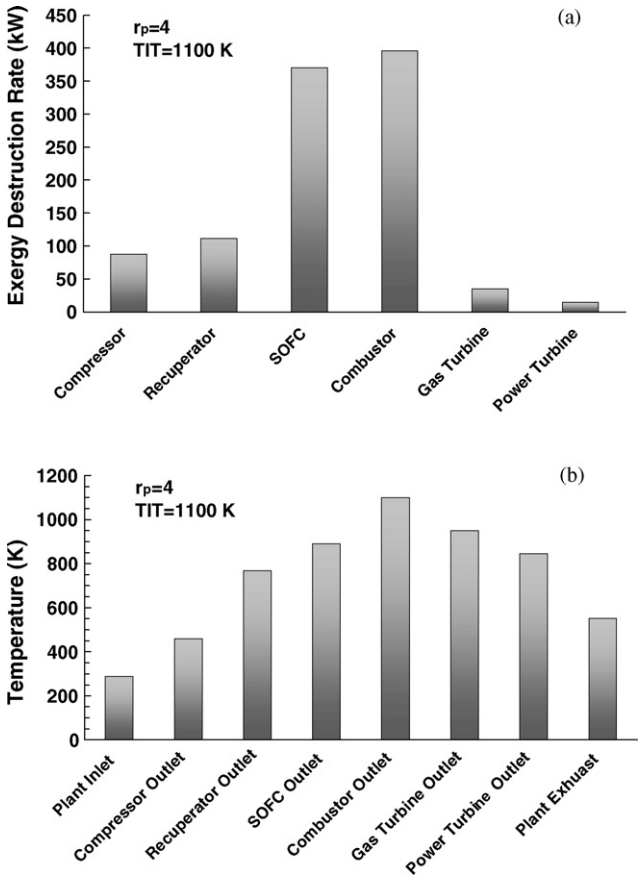

Fig. 9. Illustration of how each component of the GT–SOFC plant contributes to irreversibilities within the cycle: (a) exergy destruction rate in each component; (b) temperature distribution in the plant.

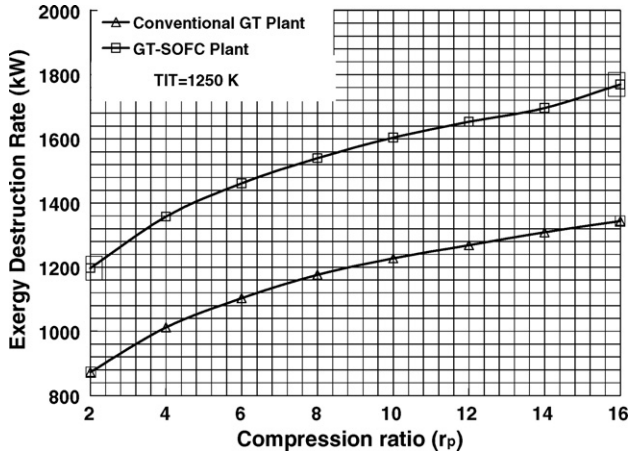

Fig. 10. Comparison of the exergy destruction rate versus the compression ratio for a gas turbine plant operation without an SOFC (conventional plant) and with an SOFC (GT–SOFC plant) at the same operation conditions.

component is first combustor, then the fuel cell and recuperator.

Further investigation has been performed to compare the performance of the GT–SOFC plant against a conventional gas turbine power plant (without including the SOFC). The results are illustrated for the exergy destruction rate and exergy efficiencies in Figs. 10–11, respectively. In the conventional GT plant, the majority of irreversibility takes place in the combustor (combustion chamber), where a large amount of heat is transferred to the working fluid, due to direct burning of the fuel. In the GT–SOFC cycle, the irreversibility within the combustor is less, when compared to a conventional plant. Nevertheless, there exists one more component, a fuel cell stack, which produces a significant rate of irreversibility, due to the chemical reaction internally. As shown in Fig. 10, the net rate of irreversibility of the GT–SOFC plant, in terms of the exergy destruction rate, is more than that of the conventional plant (approximately uniform difference). On an average basis, over the range of compression ratios presented in the figure, the exergy destruction rate of a modern plant is about 349.8 kW greater than that of a conventional plant. Despite the GT–SOFC plant having a higher rate of exergy destruction compared to the GT plant, it can be seen from Fig. 11 that it offers superior performance over a conventional cycle. The main reason is the fuel cell

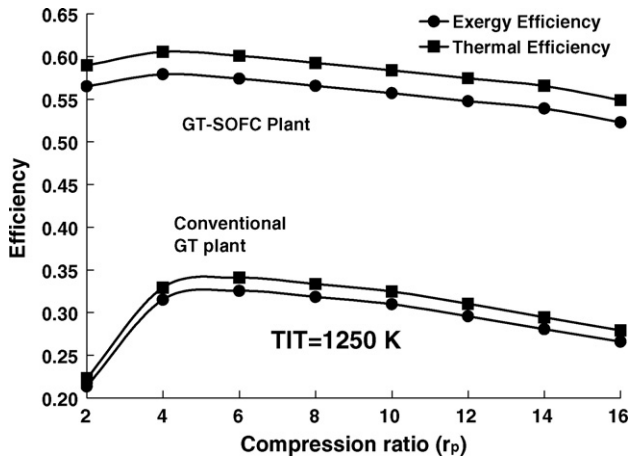

Fig. 11. Comparison of the thermal and exergy efficiencies at various compression ratios, between a gas turbine plant operation without an SOFC (conventional plant) and with an SOFC (GT–SOFC plant), at the same operation conditions.

operating at high temperatures, which allows the working fluid to be preheated before entering the combustor, as well as a considerable amount of power production. Both factors lead to higher energetic and exergetic efficiencies, compared to the conventional plant. On the other hand, from the thermal and exergy efficiency curves in Fig. 11, it can be seen that the optimal performance of a conventional GT plant occurs at a compression ratio of 6. The power requirement of a compressor in the GT plant is higher, provided both cycles operate at their optimum point, thereby having a negative role with respect to efficiency of the cycle compared to the GT–SOFC cycle. Based on the predicted values shown in Fig. 11, the GT–SOFC power plant has 26.6% better exergetic performance on an average basis than a traditional GT plant. This comparison yields 27.8% better performance of the GT–SOFC plant, with respect to thermal efficiency.

Further careful comparison in Fig. 11 reveals that the pressure ratio has a smaller effect on the combined cycle system efficiency than for a gas turbine system. This could be significant because it suggests low pressure operation does not suffer much of a penalty which could ease constraints of sealing the ceramic fuel cell components. This issue has been investigated numerically to observe the influence of pressure drop within the stack on overall system efficiency. The outcome shows that if the pressure drop within the cell stack increases by 10% (from 4%, which is considered in the analysis, to 14%), each of the thermodynamic efficiencies would decrease merely 1.4%. In an actual operating system, other losses will reduce the efficiencies. In addition to the activation, ohmic and mass transport losses of the SOFC, other issues of water management, membrane deterioration, and channel tortuosity will degrade the system performance under actual operating conditions. Cell degradation over time due to thermal loading, which leads to reduced durability of components, as well as impurities that may poison or foul the catalysts, will also further degrade the system efficiency.

4. Conclusions

In this paper, an integrated SOFC and recuperative gas turbine cycle was examined. Particular attention is given to the SOFC and combustor models. The entire cycle was treated as a lumped control volume to derive the exergy destruction rate and exergy efficiency equations. The model was verified through a comparison between results of the current model and those available in the past literature for typical operating conditions. From the simulated results, both thermal and exergy efficiencies of the GT–SOFC plant are reduced with an increase of turbine inlet temperature (TIT). These reductions are also evident from the compression ratio, after its optimum value when the cycle reaches its maximum efficiency. An increase in either the turbine inlet temperature or the compression ratio (r_p) leads to a higher rate of exergy destruction of the plant. Also, increasing the TIT improves the specific power output of the cycle. It was observed that the combustor and SOFC contribute predominantly to the total irreversibility of the system. On an average basis, over the range of compression ratios presented in the analysis, the exergy destruction rate of a modern plant is about 349.8 kW greater than that of a conventional plant. However, the GT–SOFC power plant has 26.6% better exergetic performance than a traditional GT plant. Also, there is 27.8% superior performance of a GT–SOFC plant with respect to the thermal efficiency.

Acknowledgement

The authors acknowledge the financial support provided by the Ontario Research Excellence Fund.

References

[1] H. Ide, T. Yoshida, H. Ueda, N. Horiuchi, Natural gas reformed fuel cell power generation systems-a comparison of three system efficiencies, in: Proceedings of the 24th Intersociety Energy Conversion Engineering Conference, vol. 3, Washington, DC, 1989, pp. 1517–1522.

[2] S.P. Harvey, H.J. Richter, A detailed study of a gas turbine cycle with an integrated internal reforming solid oxide fuel cell, in: Proceedings of 29th Intersociety Energy Conversion Engineering Conference, vol. 2, Monterey, CA, 1994, pp. 961–973.

[3] A.F. Massardo, F. Lubelli, Internal reforming solid oxide fuel cell-gas turbine combined cycles (IRSOFC-GT): part A—cell model and cycle thermodynamic analysis, transactions of the ASME, Journal of Engineering for Gas Turbines and Power 122 (1) (2000) 27–35.

[4] P. Costamagna, L. Magistri, A.F. Massardo, Design and part-load performance of a hybrid system based on a solid oxide fuel cell reactor and a micro gas turbine, Journal of Power Sources 96 (2) (2001) 352–368.

[5] S.H. Chan, H.K. Ho, Y. Tian, Modelling of simple hybrid solid oxide fuel cell and gas turbine power plant, Journal of Power Sources 109 (1) (2002) 111–120.

[6] S.H. Chan, H.K. Ho, Y. Tian, Multi-level modeling of SOFC–gas turbine hybrid system, International Journal of Hydrogen Energy 28 (8) (2003) 889–900.

[7] F. Calise, A. Palombo, L. Vanoli, Design and partial load exergy analysis of hybrid SOFC–GT power plant, Journal of Power Sources 158 (1) (2006) 225–244.

[8] W.J. Yang, S.K. Park, T.S. Kim, J.H. Kim, J.L. Sohn, S.T. Ro, Design performance analysis of pressurized solid oxide fuel cell/gas turbine hybrid systems considering temperature constraints, Journal of Power Sources 160 (1) (2006) 462–473.

[9] T. Araki, T. Ohba, Sh. Takezawa, K. Onda, Y. Sakaki, Cycle analysis of planar SOFC power generation with serial connection of low and high temperature SOFCs, Journal of Power Sources 158 (1) (2006) 52–59.

[10] S.K. Park, K.S. Oh, T.S. Kim, Analysis of the design of a pressurized SOFC hybrid system using a fixed gas turbine design, Journal of Power Sources 170 (1) (2007) 130–139.

[11] M. Granovskii, I. Dincer, M.A. Rosen, Performance comparison of two combined SOFC–gas turbine systems, Journal of Power Sources 165 (1) (2007) 307–314.

[12] D. Cocco, V. Tola, Comparative performance analysis of internal and external reforming of methanol in SOFC–MGT hybrid power plants, Journal of Engineering for Gas Turbines and Power 129 (2) (2007) 478–487.

[13] L. Magistri, A. Traverso, A.F. Massardo, R.K. Shah, Heat exchangers for fuel cell and hybrid system applications, Journal of Fuel Cell Science and Technology 3 (2) (2006) 111–118.

[14] K. Lobachyov, H.J. Richter, Combined cycle gas turbine power plant with coal gasification and solid oxide fuel cell, transactions of the ASME, Journal of Energy Resources Technology 118 (4) (1996) 285–292.

[15] S. Campanari, E. Macchi, Thermodynamic analysis of advanced power cycles based upon solid oxide fuel cells, gas turbines and rankine bottoming cycles, in: Proceedings of the International Gas Turbine & Aeroengine Congress & Exhibition, Stockholm, 1998.

[16] A.F. Massardo, C.F. McDonald, T. Korakianitis, Microturbine/fuel-cell coupling for high-efficiency electrical-power generation, transactions of the ASME, Journal of Engineering for Gas Turbines and Power 124 (1) (2002) 110–116.

[17] A.D. Rao, G.S. Samuelsen, A thermodynamic analysis of tubular solid oxide fuel cell based hybrid systems, transactions of the ASME, Journal of Engineering for Gas Turbines and Power 125 (1) (2003) 59–66.

[18] Y. Inui, S. Yanagisawa, T. Ishida, Proposal of high performance SOFC combined power generation system with carbon dioxide recovery, Energy Conversion and Management 44 (4) (2003) 597–609.

[19] H. Uechi, Sh. Kimijima, N. Kasagi, Cycle analysis of gas turbine–fuel cell cycle hybrid micro generation system, Journal of Engineering for Gas Turbines and Power 126 (4) (2004) 755–762.

[20] F. Calise, M. Dentice d'Accadia, A. Palombo, L. Vanoli, Simulation and exergy analysis of a hybrid solid oxide fuel cell (SOFC)–gas turbine system, Energy 31 (15) (2006) 3278–3299.

[21] T. Araki, T. Taniuchi, D. Sunakawa, M. Nagahama, K. Onda, T. Kato, Cycle analysis of low and high H_2 utilization SOFC/gas turbine combined cycle for CO_2 recovery, Journal of Power Sources 171 (2) (2007) 464–470.

[22] Y.A. Cengel, M. Boles, Thermodynamics: An Engineering Approach, 6th edition, McGraw-Hill, NY, 2007.

[23] M.C. Williams, Fuel Cell Handbook, 7th edition, EG&G Services Parsons, Inc. Science Applications International Corporation, Morgantown, WV, 2004.

[24] A. Bejan, I. Dincer, S. Lorente, A.H. Reis, A.F. Miguel, Porous Media in Modern Technologies: Energy, Electronics, Biomedical and Environmental Engineering, Springer-Verlag, New York, 2004.

[25] J. Larminie, A. Dicks, Fuel Cell Systems Explained, 2nd edition, John Wiley & Sons Ltd., West Sussex England, 2003.

[26] P. Kuchonthar, S. Bhattachary, A. Tsutsumi, Energy recuperation in solid oxide fuel cell (SOFC) and gas turbine (GT) combined system, Journal of Power Source 117 (2003) 7–13.

[27] L. Tse, F. Galinaud, R.F. Martinez-Botas, Integration of solid oxide fuel cells into a gas turbine cycle, ASME Turbo Expo Power for Land, Sea and Air, 2007, Palais Des Congres Montreal (http://www.felicitas-fuel-cells.info/files/061101_ASME2007_Tse.pdf).

[28] J. Szargut, D.R. Morris, F.R. Steward, Exergy Analysis of Thermal, Chemical and Metallurgical Processes, Hemisphere, New York, 1988.

[29] J.L. Sohn, J.S. Yang, S.T. Ro, Performance characteristics of a solid oxide fuel cell/gas turbine hybrid system with various part-load control modes, Journal of Power Sources 166 (1) (2007) 155–164.

[30] Y. Haseli, I. Dincer, G.F. Naterer, Thermodynamic modeling of a gas turbine cycle combined with a solid oxide fuel cell, International Journal of Hydrogen Energy 33 (2008) 5811–5822.

[31] A.H. Lefebvre, Gas Turbine Combustion, 2nd edition, Taylor & Francis, New York, 1999.

[32] ThomasNet, Commercial boilers maintain maximum combustion efficiency!, available at http://news.thomasnet.com/fullstory/470785, 2008.